

Electronic Supplementary Information

A new synthesis of carbon encapsulated Fe₅C₂ nanoparticles for high-temperature Fischer-Tropsch synthesis

*Seok Yong Hong, Dong Hyun Chun, Jung-Il Yang, Heon Jung, Ho-Tae Lee, Sungjun Hong, Sanha Jang, Jung Tae Lim, Chul Sung Kim, and Ji Chan Park**

Clean Fuel Laboratory, Korea Institute of Energy Research

Advanced Energy and Technology, University of Science and Technology

Department of Physics, Kookmin University

Experimental Section

Chemicals. Iron nitrate nonahydrate (Fe(NO₃)₃·9H₂O, ACS reagent, ≥98%), nickel nitrate hexahydrate (Ni(NO₃)₂·6H₂O, 99.999%), cobalt nitrate hexahydrate (Co(NO₃)₂·6H₂O, ACS reagent, ≥98%), poly (vinyl pyrrolidone) (PVP, M_w= 55,000), D-(+)-glucose (ACS reagent), activated charcoal (-100 mesh particle size, powder), and glass beads (425-600 μm size) were purchased from Aldrich. Activated carbon (powder) was obtained from Strem Chemicals Inc. The chemicals were used as received without further purification.

Synthesis of iron oxalate hydrate cube. The mixture of PVP (8.3 g, 75 mmol) and glucose (9.0 g, 50 mmol) was dissolved in 50 mL of distilled water, and then slowly heated to 100 °C for 20 min under inert condition. After that, Fe(NO₃)₃·9H₂O (10.1 g, 25 mmol), molten at 323 K, was injected into the hot PVP-glucose mixture solution at 373 K; the mixture solution was refluxed for 1 h at the same temperature. After 1 h, the colloidal dispersion was cooled to room temperature, and separated by centrifugation at 8,000 rpm for 10 min. Finally, the precipitates were washed with distilled water and ethanol several times with centrifugation at 8,000 rpm for 10 min; precipitates were dried in an oven at 333 K overnight to yield a yellowish powder.

Synthesis of iron-nickel oxalate hydrate and iron-cobalt oxalate hydrate particles. For the synthesis of nickel-iron oxalate hydrate particles, the mixture of PVP (8.3 g, 75 mmol) and glucose (9.0 g, 50 mmol) was dissolved in 50 mL of distilled water, and then slowly heated to 100 °C for 20 min under inert condition. After that, the mixed solution of $\text{Fe}(\text{NO}_3)_3 \cdot 9\text{H}_2\text{O}$ (5.1 g, 12.5 mmol) and $\text{Ni}(\text{NO}_3)_2 \cdot 6\text{H}_2\text{O}$ (3.6 g, 12.5 mmol), molten at 323 K, was injected into the hot PVP-glucose mixture solution at 373 K; the mixture solution was refluxed for 1 h at the same temperature. After 1 h, the colloidal dispersion was cooled to room temperature, and separated by centrifugation at 8,000 rpm for 10 min. Finally, the precipitates were washed with distilled water and ethanol several times by centrifugation with 8,000 rpm for 10 min; precipitates were dried in an oven at 333 K. To prepare the iron-cobalt oxalate hydrate particles, $\text{Co}(\text{NO}_3)_2 \cdot 6\text{H}_2\text{O}$ (3.6 g, 12.5 mmol) was employed with $\text{Fe}(\text{NO}_3)_3 \cdot 9\text{H}_2\text{O}$ (5.1 g, 12.5 mmol). The procedures and conditions were identical to those used in the synthesis of iron-nickel oxalate hydrate particles.

Synthesis of $\text{Fe}_5\text{C}_2@C$ catalyst. The iron oxalate hydrate powders (0.5 g) were transferred to an alumina boat in a tube-type furnace, and then heated very slowly, with a ramping rate of $0.15 \text{ K} \cdot \text{min}^{-1}$, and activated to iron carbide phase at 623 K under a CO flow of $200 \text{ mL} \cdot \text{min}^{-1}$. The sample was then thermally treated at the same temperature for 4 h under a continuous flow of CO.

Preparation of Fe/SBA-15 and Fe/AC catalysts. Mesoporous silica support SBA-15 was prepared using the hydrothermal reaction reported elsewhere. Next, using the incipient wetness method, $\text{Fe}(\text{NO}_3)_3 \cdot 9\text{H}_2\text{O}$ (1.8 g) dissolved in ethanol (5 mL) was used to saturate calcined SBA-15 powders (1.0 g). Then, the resulting powder was dried in an oven at 373 K for 24 h and calcined under an N_2 flow of $200 \text{ mL} \cdot \text{min}^{-1}$ at 673 K for 4 h. This sample was designated Fe/SBA-15. For the preparation of Fe/AC catalyst, all procedures were identical to the synthesis of Fe/SBA-15, except for the use of activated carbon powders (1.0 g) as support.

High-temperature Fischer-Tropsch synthesis. Fischer-Tropsch (FT) reactions were carried out in a fixed-bed stainless steel reactor with inner diameter of 5 mm and length of 180 mm. The Fe loading content of the $\text{Fe}_5\text{C}_2@C$ catalyst was adjusted to 20 wt% for comparison with those of Fe/SBA-15. The prepared catalyst (0.3 g) was diluted with glass

beads (3.5 g) for prevention of hot-spot generation and then placed in the fixed-bed reactor. Prior to the reaction, in the case of the Fe/SBA-15 and Fe/AC samples, in-situ activation was additionally conducted under a CO flow of 40 mL·min⁻¹ at 623 K for 4h. Then, the reaction was performed at 593 K and 15 bar for 90 h using a mixture gas (H₂/CO=1.0, GHSV=8.0 NL·g_{cat}⁻¹·h⁻¹). The flow rates of the outlet gases were measured using a wet-gas flowmeter (Shinagawa Corp.); gases were analysed using an online gas chromatograph (Agilent, 3000A Micro-GC) equipped with molecular sieve and plot Q columns. After 90 h of Fischer-Tropsch synthesis, the solid hydrocarbon products and water were collected in a cold trap at 273 K. The compositions of the wax and the liquid oil were analysed by means of an offline GC (Agilent 6890 N) using a simulated distillation method (ASTM D2887). The total and specific product yields for each sample were obtained via gas chromatography (GC) analysis of the gaseous products (C₁–C₄), and simulated distillation (SIMDIS) analysis of the isolated solid (wax) and the liquid (oil) products.

Characterization. SEM images of the samples were obtained using a Hitachi S-4800 operated at 5 kV. High resolution transmission electron microscopy (TEM) analysis was performed using a Tecnai TF30 ST and a Titan Double Cs corrected TEM (Titan cubed G2 60-300). Energy-dispersive X-ray spectroscopy (EDS) elemental mapping data were collected using a higher efficiency detection system (Super-X detector). High power powder-XRD (Rigaku D/MAX-2500, 18 kW) was also used for the analysis. XPS studies were carried out using a Sigma Probe (Thermo VG Scientific, Inc.) with a micro-focused monochromator X-ray source. The sample for XPS was prepared by placing a few drops of the colloidal solution on small pieces (5 mm × 5 mm) of gold wafer. The Fe X-ray absorption spectrum (XAS) was recorded on Beam-line 6D of the Pohang Accelerator Laboratory (PAL). The Mössbauer spectrum was obtained with a fixed absorber and a moving source. A Mössbauer spectrometer of the electromechanical type, with a 50 mCi ⁵⁷Co source in a rhodium matrix, was used in constant-acceleration mode. N₂-sorption isotherms were measured at 77 K with a Tristar II 3020 surface area analyser. Before measurement, the sample was degassed at 300 °C for 4 h under N₂ flow.

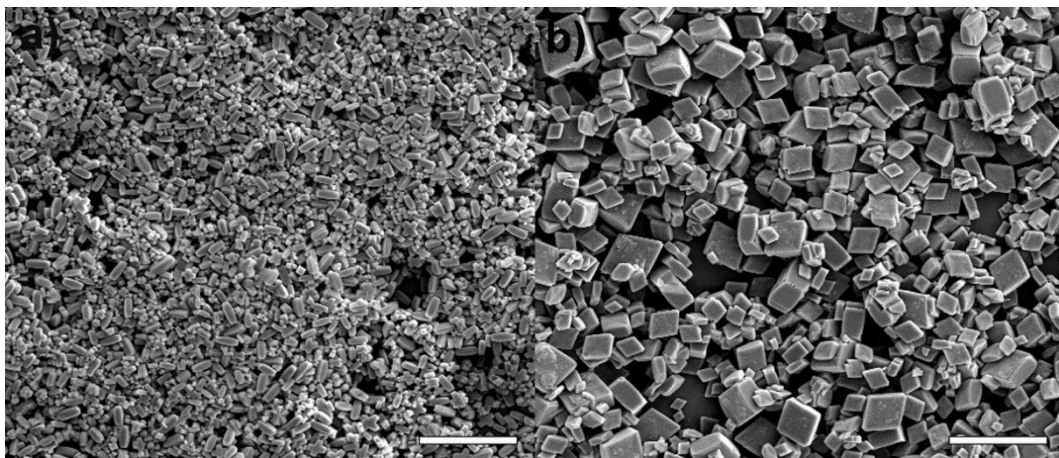


Fig. S1 SEM images of (a) iron-nickel oxalate hydrate and (b) iron-cobalt oxalate hydrate particles. All bars represent 20 μm .

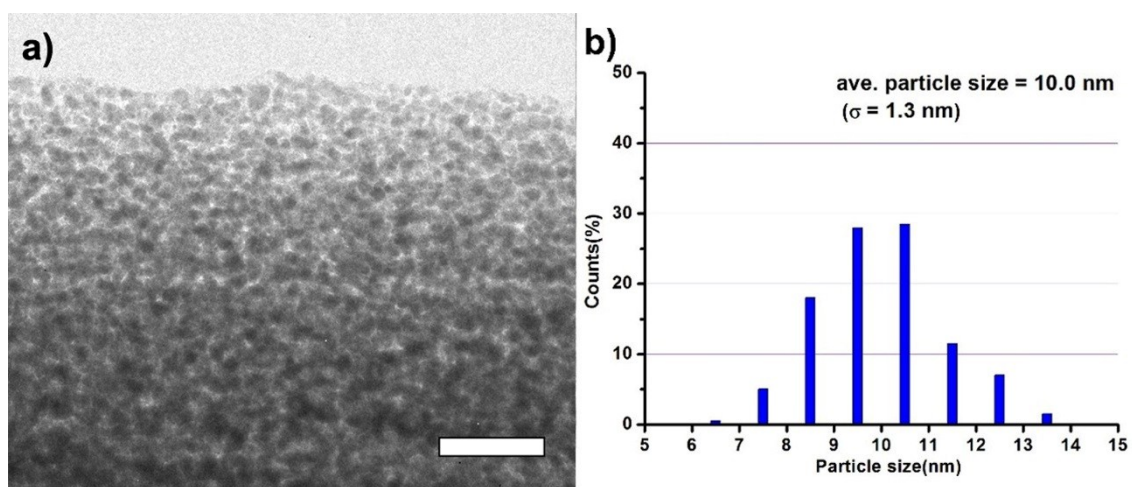


Fig. S2 TEM image and particle size distribution histogram of Fe_5C_2 nanoparticles encapsulated in carbon shells. More than 200 particles were counted. The bar (a) represents 100 nm.

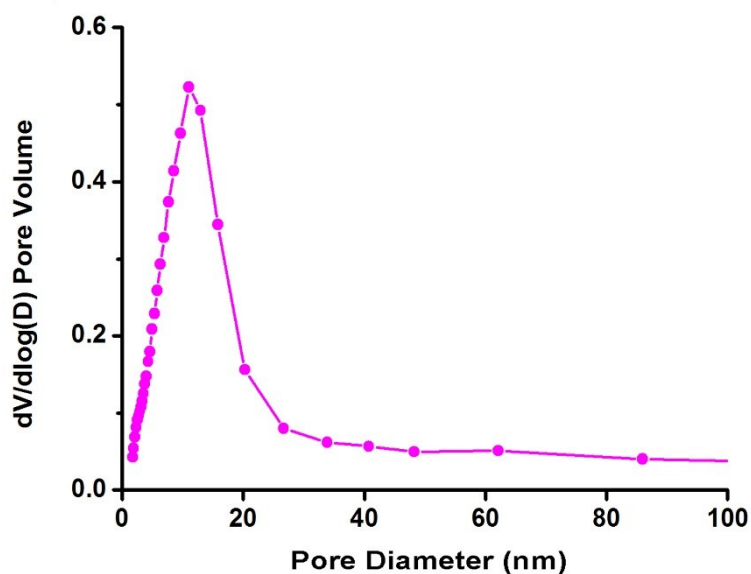


Fig. S3 Pore size distribution diagram calculated from the adsorption branch of $\text{Fe}_5\text{C}_2@\text{C}$ catalyst.

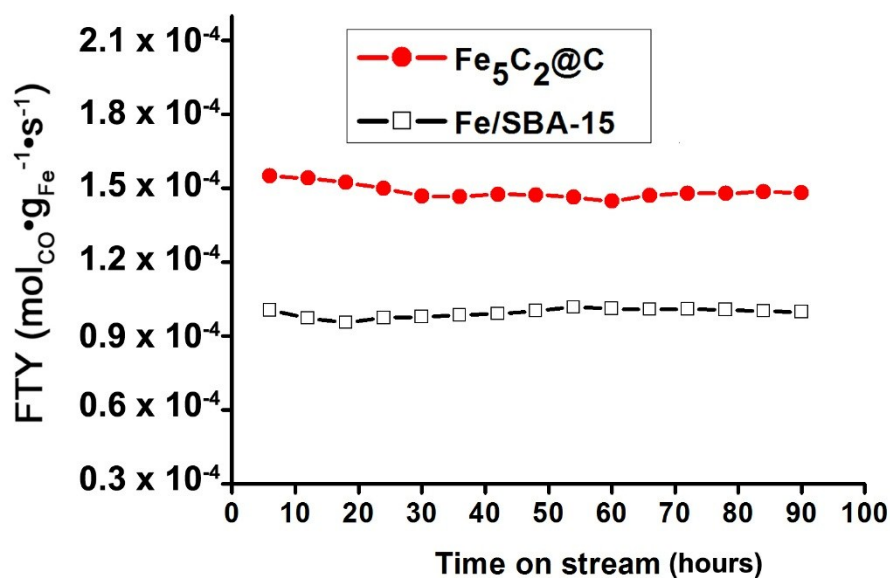


Fig. S4 Catalytic performance of $\text{Fe}_5\text{C}_2@\text{C}$ and Fe/SBA-15 catalysts for HT-FTS. The reaction tests were conducted at 320 °C, 15 bar, GHSV of $8.0 \text{ NL} \cdot \text{g}_{\text{cat}}^{-1} \cdot \text{h}^{-1}$, and an $\text{H}_2:\text{CO}$ ratio of 1.

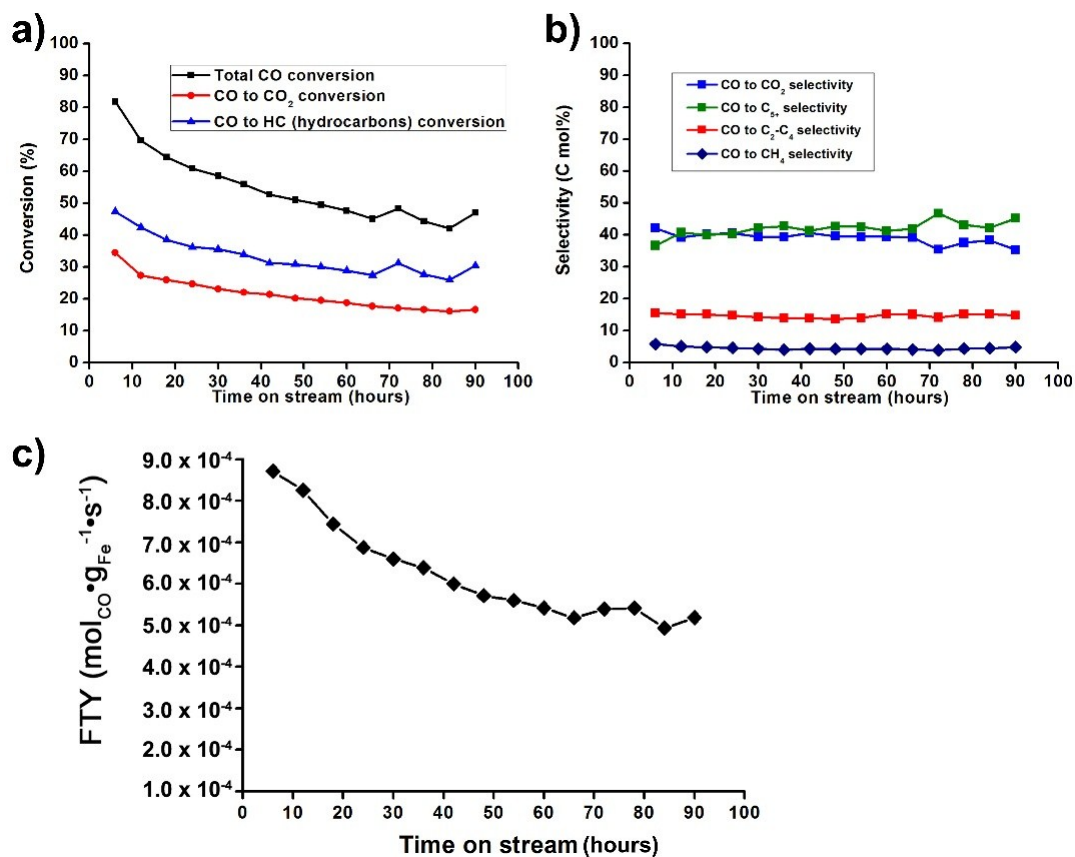


Fig. S5 (a) CO conversion, (b) hydrocarbon product selectivity data, and (c) FT activity of Fe₅C₂@C catalyst under the harsh HT-FTS reaction at 340 °C, 20 bar, GHSV of 60.0 NL·g_{cat}⁻¹·h⁻¹, and an H₂:CO ratio of 1.

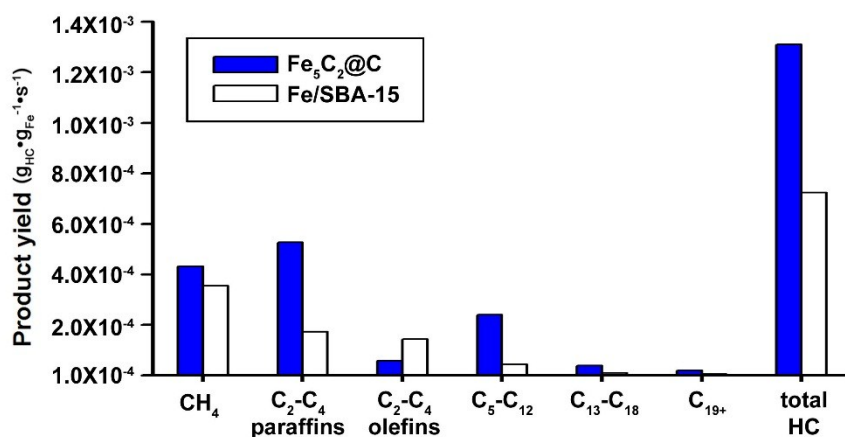


Fig. S6 Hydrocarbon product yields of Fe₅C₂@C and Fe/SBA-15 catalysts in HT-FTS. The reaction tests were conducted at 320 °C, 15 bar, GHSV of 8.0 NL•g_{cat}⁻¹•h⁻¹, and an H₂:CO ratio of 1.

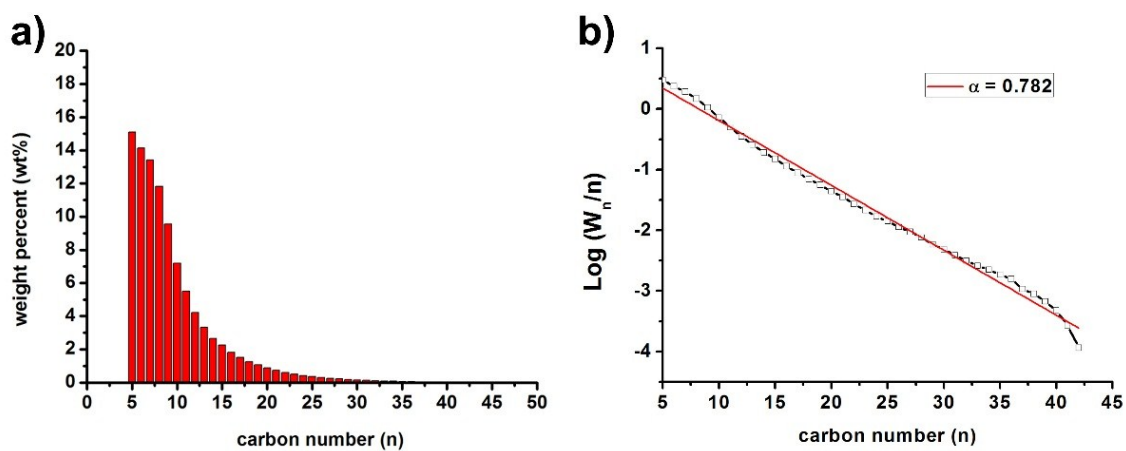


Fig. S7 (a) C₅₊ liquid hydrocarbon product distribution and (b) ASF plot and chain growth probability of Fe₅C₂@C catalyst.

Table S1. Mössbauer parameters of the Fe₅C₂@C catalyst.

Temperature (K)		site		
		Fe ₅ C ₂		
		I (8f)	II (8f)	III (4e)
295 K	H_{hf} (kOe)	213.77	176.28	105.31
	δ (mm/s)	0.15	0.06	0.07
	E_Q (mm/s)	0.00	0.04	0.05
	Area (%)	39.93	36.18	23.89
4.2 K	H_{hf} (kOe)	253.36	212.59	127.98
	δ (mm/s)	0.26	0.16	0.19
	E_Q (mm/s)	0.02	0.05	0.04
	Area (%)	37.81	44.90	17.29

H_{hf} : hyperfine magnetic field; δ : isomer shift (all the isomer shifts are referred to α -Fe at 295K); E_Q : quadrupole shift.

Table S2. Comparison of the CO conversion and FTS activity of Fe₅C₂@C catalyst with those found in the literature for Fe supported catalysts in high-temperature FTS reactions.

Catalyst	GHSV (NL·g _{cat} ⁻¹ ·h ⁻¹)	Total CO conv. (%)	FTY (mol _{CO} ·g _{Fe} ⁻¹ ·s ⁻¹)	Ref.
Fe ₅ C ₂ @C catalyst diluted with activated charcoal (Fe: 20wt%)	8.0	96	1.5 × 10 ⁻⁴	This work ^a
	12.0	84	2.0 × 10 ⁻⁴	This work ^a
	16.0	68	2.2 × 10 ⁻⁴	This work ^a
	60.0	47	5.2 × 10 ⁻⁴	This work ^c
Fe/SBA-15 (Fe: 20 wt%)	8.0	52	1.0 × 10 ⁻⁴	This work ^a
Fe/AC (Fe: 20wt%)	8.0	4.9	0.7 × 10 ⁻⁵	This work ^a
K-doped Fe ₅ C ₂ /activated charcoal (Fe: 20wt%)	8.0	94	1.5 × 10 ⁻⁴	1) ^a
10FeSi50 (Fe: 10 wt%)	16.2	33.8	2.0 × 10 ⁻⁴	2) ^b
Fe@C (Fe: 25 wt%)	60.0	59	4.9 × 10 ⁻⁴	3) ^c
Fe ₁₅ Mn ₅ /graphene (Fe: 15 wt%)	2.5	92	1.5 × 10 ⁻⁴	4) ^d
Fe/CNT (Fe: 10 wt%)	16.2	85	4.7 × 10 ⁻⁴	5) ^e
Fe/CNF (Fe: 12 wt%)	1.5	88	3.0 × 10 ⁻⁵	
Fe-Cu-K-SiO ₂ (Fe: 32 wt%)	1.5	79	1.1 × 10 ⁻⁵	6) ^f
Fe/α-Al ₂ O ₃ (Fe: 6 wt%)	1.5	77	8.5 × 10 ⁻⁵	

Catalytic tests were carried out at ^aT = 320°C, P = 15 bar, H₂/CO ratio=1, ^bT = 300°C, P = 20 bar, H₂/CO ratio=2.1
^cT = 340°C, P = 20 bar, H₂/CO ratio=1, ^dT = 325°C, P = 15 bar, H₂/CO ratio=2, ^eT = 300°C, P = 20 bar, H₂/CO
ratio=2, ^fT = 340°C, P = 20 bar, H₂/CO ratio=1.

References:

- 1) J. C. Park, S. C. Yeo, D. H. Chun, J. T. Lim, J.-I. Yang, H.-T. Lee, S. Hong, H. M. Lee, C. S. Kim and H. Jung, *J. Mater. Chem. A*, 2014, **2**, 14371.
- 2) K. Cheng, M. Virginie, V. V. Ordonsky, C. Cordier, P. A. Chernavskii, M. I. Ivantsov and A. Y. Khodakov, *J. Catal.*, 2015, **328**, 139.
- 3) V. P. Santos, T. A. Wezendonk, J. J. D. Jaén, A. I. Dugulan, M. A. Nasalevich, H.-U. Islam, A. Chojecki, S. Sartipi, X. Sun, A. A. Hakeem, A. C.J. Koeken, M. Ruitenbeek, T. Davidian, G. R. Meima, G. Sankar, F. Kapteijn, M. Makkee and J. Gascon, *Nat. Commun.*, 2015, **6**, 6451.
- 4) S. O. Moussa, L. S. Panchakarla, M. Q. Ho and M. S. El-Shall, *ACS Catal.* 2014, **4**, 535.
- 5) V. V. Ordonsky, B. Legras, K. Cheng, S. Paul and A. Y. Khodakov, *Catal. Sci. Technol.*, 2015, **5**, 1433.
- 6) H. M. T. Galvis, J. H. Bitter, C. B. Khare, M. Ruitenbeek, A. I. Dugulan and K. P. de Jong, *Science*, 2012, **335**, 835.